

Theory on polarization-averaged core-level molecular-frame photoelectron angular distributions: II. Extracting the X-ray induced fragmentation dynamics of carbon monoxide dication from forward and backward intensities

Fukiko Ota, Keisuke Hatada, Didier Sébilleau, Kiyoshi Ueda, Kaoru Yamazaki

▶ **To cite this version:**

Fukiko Ota, Keisuke Hatada, Didier Sébilleau, Kiyoshi Ueda, Kaoru Yamazaki. Theory on polarization-averaged core-level molecular-frame photoelectron angular distributions: II. Extracting the X-ray induced fragmentation dynamics of carbon monoxide dication from forward and backward intensities. Journal of Physics B: Atomic, Molecular and Optical Physics, 2021, 54 (8), pp.084001. 10.1088/1361-6455/abcfd8 . hal-03103805

HAL Id: hal-03103805

https://univ-rennes.hal.science/hal-03103805

Submitted on 15 Jun 2021

HAL is a multi-disciplinary open access archive for the deposit and dissemination of scientific research documents, whether they are published or not. The documents may come from teaching and research institutions in France or abroad, or from public or private research centers.

L'archive ouverte pluridisciplinaire **HAL**, est destinée au dépôt et à la diffusion de documents scientifiques de niveau recherche, publiés ou non, émanant des établissements d'enseignement et de recherche français ou étrangers, des laboratoires publics ou privés.

Theory on polarization-averaged core-level molecular-frame photoelectron angular distributions: II. Extracting the X-ray induced fragmentation dynamics of carbon monoxide dication from forward and backward intensities

F Ota[1], K Hatada[2], D Sébilleau[3], K Ueda[4] and K Yamazaki[5,6]

[1] Graduate School of Science and Engineering for Education, University of Toyama, Gofuku 3190, Toyama 930-8555, Japan
[2] Faculty of Science, Academic Assembly, University of Toyama, Gofuku 3190, Toyama 930-8555, Japan
[3] Département Matériaux Nanosciences, Institut de Physique de Rennes, UMR UR1-CNRS 6251, Université de Rennes, F-35000 Rennes, France
[4] Institute of Multidisciplinary Research for Advanced Materials, Tohoku University, Katahira 2-1-1, Aoba-ku, Sendai 980-8577, Japan
[5] Institute for Materials Research, Tohoku University, 2-1-1 Katahira, Aoba-ku, Sendai 980-8577, Japan
[6] Attosecond Science Research Team, Extreme Photonics Research Group, RIKEN Center for Advanced Photonics, RIKEN, 2-1 Hirosawa, Wako, Saitama, 351-0198, Japan.

E-mail: hatada@sci.u-toyama.ac.jp, kaoru.yamazaki@riken.jp

Abstract. Recent developments in high repetition-rate X-ray free electron lasers (XFELs) such as the European XFEL and the LSCS-II, combined with coincidence measurements at the COLTRIMS–Reaction Microscope, is now opening a door to realize the long-standing dream to create molecular movies of photo-induced chemical reactions in gas-phase molecules. In this paper, we propose a new theoretical method to experimentally visualize the dissociation of diatomic molecules via time-resolved polarization-averaged molecular-frame photoelectron angular distributions (PA-MFPADs) measurements using the COLTRIMS–Reaction Microscope and the two-color XFEL pump-probe set-up. We used first and second order scattering theory within the Muffin-tin approximation, which is valid for a sufficiently high kinetic energy of photoelectron, typically above 100 eV, and for long bond lengths. This leads to a simple EXAFS-type formula for the forward and backward scattering peaks in the PA-MFPADs structure. This formula relies only on three semi-empirical parameters obtainable from the time-resolved measurements. It can be used as a "bond length ruler" on experimental results. The accuracy and applicability of the new ruler equation are numerically examined against the PA-MFPADs of CO^{2+} calculated with Full-potential multiple scattering theory as a function of the C-O bond length reported in the preceding work [1]. The bond lengths retrieved from the the PA-MFPADs via our EXAFS-like formula coincide within an accuracy of 0.1 Å with the original C-O bond lengths used in the reference *ab-initio* PA-MFPADs. We expect time-resolved PA-MFPADs to become a new attractive tool to make molecular movies visualizing intramolecular reactions.

Keywords: PA-MFPADs, Multiples Scattering theory, Coincidence measurement, FEL

Submitted to: *J. Phys. B: At. Mol. Opt. Phys.*

ACCEPTED MANUSCRIPT

1. Introduction

Visualizing structural changes of molecules in reactions in real time has been a long-standing dream in chemical physics, physical chemistry, and biochemistry [2, 3]. In particular, seeing structural changes of photoexcited free molecules is of fundamental interest but it is still a challenge. The advent of X-ray free electron lasers (XFEL) delivering extremely short X-ray pulses down to a few femtoseconds [4] and of a mega-electron-volt ultrafast electron diffraction (UED) system [5] at SLAC opens up new pathways to investigate these structural changes in real time [6, 7].

As an alternative approach, time-resolved photoelectron diffraction (PED) employing an XFEL as a photoionizing source was recently proposed [8, 9]. PED is a technique well-established as an analytic tool in surface science [10], where the directions of core-level photoelectrons emitted from a specific site are measured with respect to the sample orientation. In the gas-phase PED experiments, the molecular axis needs to be fixed in space. In case of synchrotron radiation experiments, this may be realized by detecting fragment ions in a momentum-resolved manner and core-level photoelectrons are then measured in coincidence with these fragment ions, using a COLTRIMS–Reaction Microscope [11]. These measurements provide us with photoelectron angular distributions in molecular frame (MFPADs), which are equivalent to PED. Indeed, extractions of the three dimensional structure defined by the direction of the bonds [12] and the bond length [13] from the measured polarization-averaged MFPADs (PA-MFPADs) have been demonstrated.

Some attempts towards time-resolved MFPADs measurements with XFELs were reported [14, 15, 16, 17] but there has been no report on time-resolved studies of molecular structural changes so far, due to complexity of the time-resolved MFPADs measurements with XFELs. Coincidence experiments to measure MFPADs using synchrotron radiation as a light source are well established, but up to now, they were practically impossible with a low repetition-rate XFELs as three different lasers, one for actively arraying the molecule in space, one for exciting the molecule to initiate a reaction, and the XFEL as a light source for the MFPADs measurements, had to be operated in a synchronized manner [14] in order to perform the experiment.

The first high repetition-rate XFEL, the European XFEL [18], has just started operating for users. Its high repetition-rate opens up the door to coincidence experiments with the COLTRIMS–Reaction Microscope routinely used for MFPADs measurements, and Kastirke *et al.* [19] have just reported the first successful implementation of this technique at the soft X-ray beam line of the European XFEL. In the USA, LCLS-II will soon start operating with a high repetition-rate in the soft to tender X-ray regions [20]. Furthermore, two-color XFEL operations will be available at the European XFEL [21] and at the LCLS-II [20], allowing to perform pump-probe experiment for multiple edges scheme such as C(1s) pump O(1s) probe etc. These two-color operations combined with the COLTRIMS–Reaction Microscope will provide the scientific community with another attractive pathway to make molecular movies to visualize the intramolecular reaction occurring, e.g., in dicationic states.

In the present work, we consider the process where the first XFEL pulse produces CO^{2+} via the Auger decay that follows the core ionization of CO, and the second XFEL pulse kicks out an oxygen $1s$ electron from CO^{2+}. Using first and second order Muffin-tin multiple scattering theory, we derive analytical EXAFS-type expressions for the backward-forward scattering peaks. Employing the Full-potential multiple scattering PA-MFPADs data reported in the preceding paper [1], we introduce a parameterized formula to describe the EXAFS-like oscillations in the forward-backward intensity ratio. This formula relies only on three semi-empirical parameters that account for the effects of Full-potential multiple scattering on the PA-MFPADs. Because of it simplicity, it can be used to extract the bond length from the experimental PA-MFPADs, which varies as a function of pump-probe delay.

2. Analytical Expression for PA-MFPADs to Study Dynamics of Dissociating CO^{2+}

In this section, we derive analytical formulas to extract the C-O bond length during the dissociation process. We first calculate the PA-MFPADs within our Full-potential multiple scattering theory in order to monitor the variations in the PA-MFPADs patterns with the changing C-O bond length. The details of the theory are found in the preceding paper [1]. Then, in Section 2.3, we derive analytical expressions for the ratio of the backward-intensity to forward-intensity s a function of the C-O bond length, using the single-scattering Plane Wave approximation within the Muffin-tin approximation.

2.1. Numerical Results of PA-MFPADs with Full-potential Multiple Scattering Theory for Dissociating CO^{2+}

ACCEPTED MANUSCRIPT

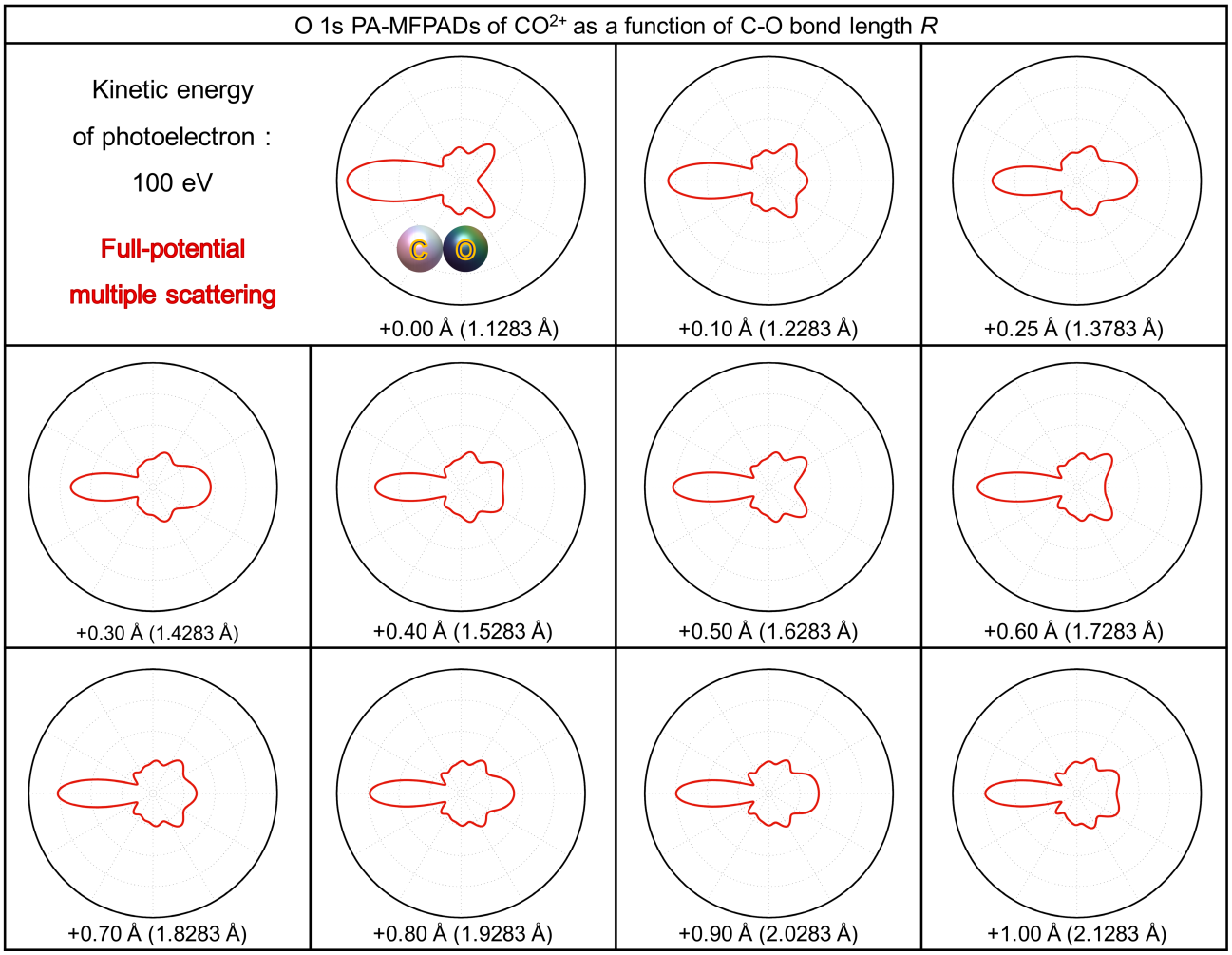


Figure 1. The oxygen 1*s* PA-MFPADs of CO^{2+} calculated with the Full-potential multiple scattering method as a function of the C-O bond length R in Å. Here, the photoelectron energy is 100 eV. More details are provided in the preceding paper [1].

In order to compute the PA-MFPADs for a photoelectron of momentum $\mathbf{k}$, we use the formula

$$\langle I(\mathbf{k})\rangle_\varepsilon = \frac{8\pi^2\alpha\hbar\omega}{3}\sum_{n=-1}^{1}\sum_{m_c}\left|\sqrt{\frac{4\pi}{3}}\sum_{LL'}B_L^{i*}(\mathbf{k}) \times C(L,1n,L_c)\int dr\, r^3\, R_{L'L}(r;k)\, R^c_{L_c}(r)\right|^2, \quad (1)$$

where

$$B_L^{i*}(\mathbf{k}) = = \sum_{jL'}\tau^{ij}_{LL'}\, I^j_{L'}(\mathbf{k}), \quad (2)$$

and

$$\tau \equiv \left(T^{-1}-G\right)^{-1} = T\,(1-GT)^{-1}, \quad (3)$$

$$I^i_L(\mathbf{k}) \equiv \sqrt{\frac{k}{\pi}}\, e^{i\mathbf{k}\cdot\mathbf{R}_{io}}\mathcal{Y}_L(\hat{\mathbf{k}}). \quad (4)$$

i and j identify the scattering sites. α is the fine structure constant, $\mathbf{R}_{io}$ is the vector connecting the origin to the center of scattering site i and the $\mathcal{Y}_L$ are the real spherical harmonics with angular momentum $L = (l,m)$. In the second line of equation 1, $C(L,1n,L_c)$ is a Gaunt coefficient with real spherical harmonics and the integral is the radial integral between the local solution and the core wave function. In equation 3, T is the transition operator (or scattering T matrix) and G is the KKR structure factor [22, 23]. More details are reported in our preceding paper [1].

Figure 1 depicts the PA-MFPADs calculated as a function of the C-O bond length R. The calculations have been performed with our Full-potential multiple scattering method. The electron charge density was computed at the RASPT2/ANO-RCC-VQZP level of theory as implemented in MOLCAS 8.2 [24] for the major excited state $1\sigma^{-1}5\sigma^{-2}$ (i.e. O $1s^{-1}$ HOMO^{-2}) of the Auger final state [25]. The kinetic energy of photoelectron was set to 100 eV, where energies are counted from the interstitial potential V_0, which itself is defined as the average of the potential of the scattering cells. We note that the forward-intensity peak towards

ACCEPTED MANUSCRIPT

the carbon atom has a large lobe due to the focusing effect. The backward-intensity peak lobe in the opposite direction oscillates as a function of R. These oscillations correspond to the EXAFS oscillations. Therefore, the shape of the PA-MFPADs contains certainly the information about the bond length. We will hereafter derive analytical EXAFS-like formulas that can be used to extract the C-O bond length from the PA-MFPADs.

2.2. Single and Double Scattering Approximations with the Muffin-tin Approximation

In this subsection, we derive the PA-MFPADs intensity within the Muffin-tin approximation, in which the electrostatic potential and the charge density are spherically averaged on each scattering site, thereby neglecting their anisotropies. This will allow us in the following subsections to analytically study the relationship between the PA-MFPADs patterns and the C-O bond length.

In the framework of the Muffin-tin approximation, the radial part of local solution $R_{LL'}(r_i;k)$ and the transition matrix $T^i_{LL'}$ are diagonal in angular momentum,

$$R_{LL'}(r_i;k) \to R_l(r_i;k)\,\delta_{LL'} \tag{5}$$

$$T^i_{LL'} \to T^i_l\,\delta_{LL'} \tag{6}$$

Consequently, the intensity of the PA-MFPADs becomes

$$\begin{aligned}\langle I(\mathbf{k})\rangle_\varepsilon \;\sim\; & \frac{8\pi^2\alpha\hbar\omega}{3}\sum_{n=-1}^{1}\sum_{m_c}\left|\sqrt{\frac{4\pi}{3}}\sum_L B^{i*}_L(\mathbf{k})\right.\\ & \left.\times\, C(L,1n,L_c)\int dr\, r^3\, R_l(r;k)\, R^c_{L_c}(r)\right|^2\\ =\; & \frac{8\pi^2\alpha\hbar\omega}{3}\sum_{n=-1}^{1}\sum_{m_c}\left|\sqrt{4\pi}\sum_L B^{i*}_L(\mathbf{k})\, C(L,1n,L_c)\, M^l_{L_c}\right|^2\end{aligned} \tag{7}$$

where $M^l_{L_c} \equiv \sqrt{1/3}\int dr\, r^3\, R_l(r;k)\, R^c_{L_c}(r)$ is the transition matrix describing the excitation of the photoelectron. We specialize now in the photoemission from an oxygen $1s$ core orbital, $L_c = (0,0)$, so that

$$\langle I(\mathbf{k})\rangle_\varepsilon \;\sim\; \frac{8\pi^2\alpha\hbar\omega}{3}\left|M^1_{00}\right|^2\sum_{n=-1}^{1}\left|B^i_{1n}(\mathbf{k})\right|^2. \tag{8}$$

For a sufficiently high kinetic energy of photoelectron and a long bond length, namely a large value of kR, the spectral radius of matrix GT in equation 3 becomes less than one, i.e. $\rho(GT) < 1$ [26]. Under this condition, we can expand the multiple scattering matrix τ into a series expansion ,

$$\tau = T\,(1-GT)^{-1} \approx T + TGT + TGTGT + \cdots. \tag{9}$$

The first term corresponds to the direct photoemission process on the absorbing atom and the second term includes all the scattering paths contributing to the single-scattering process. In the same way the higher terms describe the higher scattering orders.

In order to help the understanding of the PA-MFPADs, we introduce a further simplification into our equations, replacing the KKR structure factors $G^{ij}_{LL'}$ by their plane wave approximation [27],

$$G^{ij}_{LL'} \;\sim\; -4\pi\, i^{l-l'}\,\frac{e^{ikR_{ij}}}{R_{ij}}\mathcal{Y}_L(\hat{\mathbf{R}}_{ij})\,\mathcal{Y}_{L'}(\hat{\mathbf{R}}_{ij}), \tag{10}$$

which is valid for long bond lengths and small size atoms.

Since the CO molecule has infinite symmetry around the molecular axis ($C_{\infty v}$ point group), the intensity depends solely on the norm k and polar angle θ of vector $\mathbf{k}$, i.e. $\langle I(\mathbf{k})\rangle_\varepsilon = \langle I(k,\theta)\rangle_\varepsilon$.

Making use of these additional approximations, we obtain the following formula for the PA-MFPADs within the Muffin-tin plane wave single-scattering approximation,

$$\begin{aligned}\left\langle I_{single}(k,\theta)\right\rangle_\varepsilon &= 2k\alpha\hbar\omega\left|T_1^{\,O}\,M^1_{00}\right|^2\\ &\times\left\{1+\frac{2\Re\left(e^{ikR(1-\cos\theta)}f^{\,C}(k,\theta)\right)}{R}\cos\theta+\frac{\left|f^{\,C}(k,\theta)\right|^2}{R^2}\right\}\end{aligned} \tag{11}$$

where $f^{\,C}(k,\theta) \equiv -4\pi\sum_L T^C_l\,\mathcal{Y}_L(\hat{\mathbf{k}})\,\mathcal{Y}_L(\hat{\mathbf{r}})$ is the scattering amplitude and the superscripts identify the scattering atom, i.e. C for carbon and O for oxygen. The first term corresponds to the direct photoemission process in which the electron does not suffer any subsequent scattering after its excitation from a core state to the continuum state. Because of the polarization averaging, this term brings no angular dependency in the PA-MFPADs. The third term describes the single scattering by the carbon atom. The second term corresponds to the interference between the direct and singly scattered waves. It is this latter term which creates the so-called *flower shape* at intermediate angles.

In the case of double-scattering, the PA-MFPADs intensity becomes

$$\begin{aligned}&\langle I_{double}(k,\theta)\rangle_\varepsilon = 2k\alpha\hbar\omega\,\left|\,T_1^{\,O}M^1_{00}\right|^2\\ &\times\left\{1+\frac{\left|f^{\,C}(k,\theta)\right|^2}{R^2}+\frac{\left|f^{\,O}(k,\pi-\theta)\,f^{\,C}(k,\pi)\right|^2}{R^4}\right.\\ &\quad+\frac{2\Re\left(e^{ikR(1-\cos\theta)}\,f^{\,C}(k,\theta)\right)}{R}\cos\theta\\ &\quad+\frac{2\Re\left(e^{2ikR}\,f^{\,O}(k,\pi-\theta)\,f^{\,C}(k,\pi)\right)}{R^2}\cos\theta\\ &\quad\left.+\frac{2\Re\left(e^{ikR(1+\cos\theta)}\,f^{*C}(k,\theta)\,f^{\,O}(k,\pi-\theta)\,f^{\,C}(k,\pi)\right)}{R^3}\right\}.\end{aligned} \tag{12}$$

Compared to the single scattering case, we see the appearance of three new terms, the third, fifth and sixth terms. The order of R in the denominator reflects the propagation of the photoelectron, the higher this order, the smaller its contribution. The third term is a purely double scattering intensity term. The fifth term corresponds to the interference between the direct and doubly scattered waves, and the sixth term is the single-double scattering interference term.

ACCEPTED MANUSCRIPT

2.3. Forward- and Backward-intensities as a Function of the Bond Length : EXAFS-like Formulas

The forward ($\theta = 0$)- and backward ($\theta = \pi$)- intensities for single scattering are,

$$\left\langle I_{single}(k,0)\right\rangle_{\varepsilon} = 2k\alpha\hbar\omega \left| T_1^{\,O} M_{00}^{1} \right|^2 \times \left\{ 1 + \frac{2\Re\left(f^{C}(k,0)\right)}{R} + \frac{\left|f^{C}(k,0)\right|^2}{R^2} \right\}, \tag{13}$$

$$\left\langle I_{single}(k,\pi)\right\rangle_{\varepsilon} = 2k\alpha\hbar\omega \left| T_1^{\,O} M_{00}^{1} \right|^2 \times \left\{ 1 - \frac{2\Re\left(e^{2ikR} f^{C}(k,\pi)\right)}{R} + \frac{\left|f^{C}(k,\pi)\right|^2}{R^2} \right\}. \tag{14}$$

In this case, only the backward-intensity $\left\langle I_{single}(k,\pi)\right\rangle_{\varepsilon}$ oscillates as a function of kR. For double scattering, the forward ($\theta = 0$) and backward ($\theta = \pi$) intensities become,

$$\begin{aligned}\langle I_{double}(k,0)\rangle_{\varepsilon} &= 2k\alpha\hbar\omega \left| T_1^{\,O} M_{00}^{1} \right|^2 \\ &\times \left\{ 1 + \frac{\left|f^{C}(k,0)\right|^2}{R^2} + \frac{\left|f^{O}(k,\pi)\, f^{C}(k,\pi)\right|^2}{R^4} \right. \\ &+ \frac{2\Re\left(f^{C}(k,0)\right)}{R} + \frac{2\Re\left(e^{2ikR}\, f^{O}(k,\pi)\, f^{C}(k,\pi)\right)}{R^2} \\ &\left. + \frac{2\Re\left(e^{2ikR}\, f^{*C}(k,0)\, f^{O}(k,\pi)\, f^{C}(k,\pi)\right)}{R^3} \right\}, \end{aligned} \tag{15}$$

$$\begin{aligned}\langle I_{double}(k,\pi)\rangle_{\varepsilon} &= 2k\alpha\hbar\omega \left| T_1^{\,O} M_{00}^{1} \right|^2 \\ &\times \left\{ 1 + \frac{\left|f^{C}(k,\pi)\right|^2}{R^2} + \frac{\left|f^{O}(k,0)\, f^{C}(k,\pi)\right|^2}{R^4} \right. \\ &- \frac{2\Re\left(e^{2ikR}\, f^{C}(k,\pi)\right)}{R} - \frac{2\Re\left(e^{2ikR}\, f^{O}(k,0)\, f^{C}(k,\pi)\right)}{R^2} \\ &\left. + \frac{2\Re\left(f^{*C}(k,\pi)\, f^{O}(k,0)\, f^{C}(k,\pi)\right)}{R^3} \right\}. \end{aligned} \tag{16}$$

Now, the forward-intensity also oscillates with $2kR$. These equations may explain the trends of the PA-MFPADs.

From an experimental point of view, it is significantly easier to extract the variation of the ratio of the backward- and forward-intensities rather than the intensity variations of the backward- and forward-intensities themselves. So, we consider their ratio now. Figure 2 depicts the intensity ratio of the forward- and backward-intensity peaks of the oxygen 1*s* PA-MFPADs of CO^{2+} as a function of the C-O bond length R from 1.1283 Å (equilibrium bond length in the ground state) to 2.1283 Å. They were obtained from our Full-potential multiple scattering calculations [1]. We see clearly here the EXAFS-like oscillations in the ratio. In order to model these oscillations with an analytical formula, we employ the single-scattering approximation, which is known to capture the EXAFS oscillations:

$$\begin{aligned}\eta(k,R) &\equiv \frac{\left\langle I_{single}(k,\pi)\right\rangle_{\varepsilon}}{\left\langle I_{single}(k,0)\right\rangle_{\varepsilon}} \\ &= \frac{a(k,R)}{R}\cos(2kR - \phi^{C}(k,\pi)) + b(k,R), \end{aligned} \tag{17}$$

where

$$a(k,R) \equiv -\frac{2R^2\left|f^{C}(k,\pi)\right|}{R^2 + 2R\,\Re\left(f^{C}(k,0)\right) + \left|f^{C}(k,0)\right|^2}, \tag{18}$$

$$b(k,R) \equiv \frac{R^2 + \left|f^{C}(k,\pi)\right|^2}{R^2 + 2R\,\Re\left(f^{C}(k,0)\right) + \left|f^{C}(k,0)\right|^2}. \tag{19}$$

The ratio of the backward-intensity against the forward-intensity oscillates with a frequency $2kR$. The function $\phi(k,\pi)$ is the phase factor of the back scattering amplitude from the carbon atom, $f^{C}(k,\pi) = \left|f^{C}(k,\pi)\right| \exp\left[i\phi^{C}(k,\pi)\right]$.

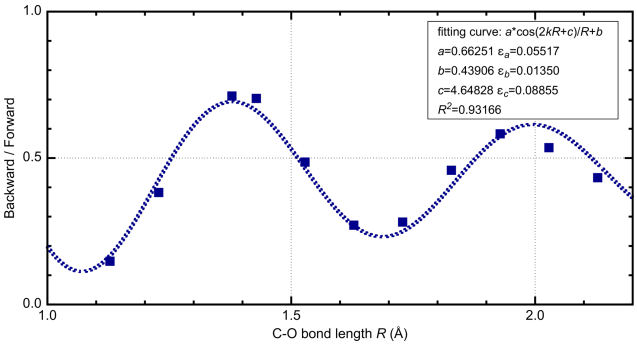


Figure 2. Ratio of the backward-intensity to the forward-intensity of the oxygen 1*s* PA-MFPADs of CO^{2+} as a function of the C-O bond length R from 1.1283 Å (equilibrium bond length in the ground state) to 2.1283 Å for the $1\sigma^{-1}5\sigma^{-2}$ state, calculated with the Full-potential multiple scattering method (Blue dot) and compared to our least square fitted result using equation 17 (dashed line).

3. Extraction of the Bond Length Information from the Forward-Backward Peaks in the PA-MFPADs

In this section, we propose a new experimental procedure to determine the time evolution of the bond length of diatomic molecules. This procedure is based on the approximation of $\eta(k,R)$ given by equation 17.

We begin by noting that $a(k,R)$, $b(k,R)$ and $\phi^{C}(k,\pi)$ vary slowly as a function of R in equation 17. Therefore, we may consider them as constant. As a consequence, the forward-backward intensity ratio $\eta(k,R)$ can be adequately fitted by the EXAFS-like equation

$$\eta(k,R) = \frac{a}{R}\cos(2kR - \phi)) + b. \tag{20}$$

In figure 2, we show the comparison between this equation with a least square fitting and the theoretical data calculated

ACCEPTED MANUSCRIPT

with our Full-potential multiple scattering theory. Here the correlation coefficient is $r^2 = 0.93166$, suggesting that our fitting of a, b and ϕ is reasonable. This means that our equation of $\eta(k, R)$ works as an experimental "bond length ruler".

In figure 3, we have plotted the deviation of the C-O bond length at the peak positions of $\eta(k, R)$ against that of our Full-potential calculations obtained by numerical differentiation. The accuracy of the extracted bond length R employing equation 20 is estimated to be better than 0.1 Å as shown in figure 3 (root mean square error: 0.032 Å). The error on the C-O bond length ΔR is a linear function of the original C-O bond length R_{Original}: $\Delta R = 0.12472 R_{\text{Original}} - 1.9310$ (correlation coefficient $r^2 = 1.00$). The upper bound of the relative error $\Delta R / R_{\text{Original}}$ is estimated to be 12.5 % in the limit of sufficiently large C-O bond lengths.

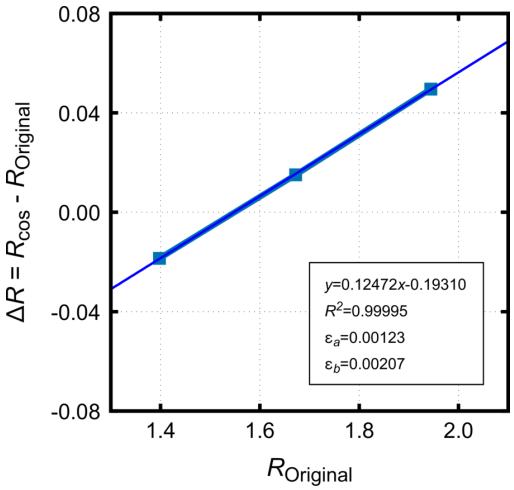


Figure 3. The deviation of the C-O bond length evaluated from the fitting of equation 17 against the Full-potential calculations displayed in figure 2.

The major origin of the fitting error in R comes for the neglect of the variations of a, ϕ, and b (see equations 17-19). We have also neglected the chemical shift of k, which can be estimated to 2-3 % from our RASPT2/ANO-RCC-VQZP results as detailed in the preceding paper [1]. In addition, equation 17 does not contain the multiple scattering (second order terms in equations 15 and 16, and other higher order terms) included in our Full-potential multiple scattering calculations. These additional terms will modulate the phase of the EXAFS-like fitting in equation 20 and explain the small error induced by our ruler formula on the C-O bond length.

Experimentally, one can measure the ratio $\eta(k, R)$ between the forward- and backward-intensities of the PA-MFPADs with a COLTRIMS–Reaction Microscope. Below, we describe other detection schemes combining impulsive orientation of the molecule [28]. The orientation of linear molecules that have dipole moments may be prepared by the phase controlled two $\omega - 2\omega$ pulses, say, at 800 nm and 400 nm [29]. Orientating CO molecules in space, one can measure $\eta(k, R)$ with two electron time-of-flight (TOF) spectrometers placed face to face in the direction of the axis of parallel polarization of four sequential pulses, as shown in figure 4. This tandem TOF apparatus is often used for the carrier envelope phase measurements of femtosecond/attosecond optical pulses and referred to as stereo-ATI [30]. Alternatively, one can use a velocity map imaging (VMI) [17] electron spectrometer instead of two TOF spectrometers. These approaches may also work for low repetition-rate XFELs [17] or high-power high-harmonic generation light sources [31] as long as two color X-ray pulses are available. For these forward-backward photoemission measurements of molecules with the maximally oriented rotational wave packet, the jitters between the optical lasers and pump and probe X-ray pulses may need to be corrected [32, 33, 34] by the shot-by-shot monitoring technique, which has already been implemented in the XFEL facilities.

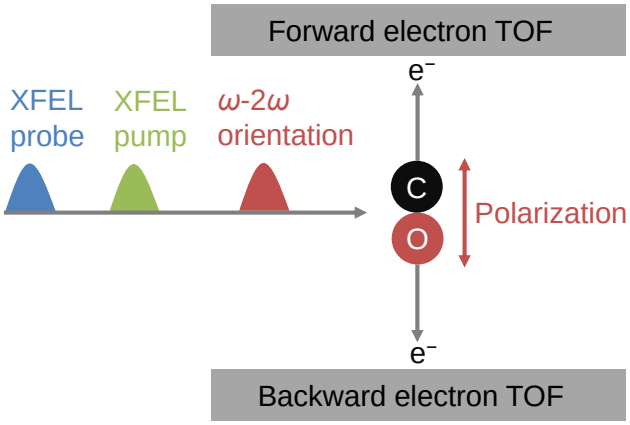


Figure 4. A schematic description of an experimental set-up for the forward-/backward-intensity ratio measurements without COLTRIMS–Reaction Microscope. Here the forward-/backward-intensities are measured for molecules spatially oriented impulsively by the phase-coherent two-color (e.g., 800 nm and 400 nm) double pulses, in the direction parallel to the molecular orientation that coincides with the linear polarization axis of the two XFEL pulses. Although polarization average is not taken in this scheme, the ratio thus obtained coincides with $\eta(k, R)$ defined in equation 17.

4. Conclusions

In this work, we have proposed a new theoretical method to extract from the experimental data the dissociation dynamics of diatomic molecules via time-resolved PA-MFPADs measurements using the COLTRIMS–Reaction Microscope and a two-color XFEL pump-probe set-up. The Muffin-tin single scattering approximation leads to the simple EXAFS-like formula of equation 17. This formula acts as an experimental "bond length ruler" controlled by only three parameters related to experimental results. In

ACCEPTED MANUSCRIPT

this study we have only considered the case of a two atom molecule. However, our method is also valid for polyatomic molecules where EXAFS-like oscillations are also present. At lower energies this simple single scattering picture will break down and multiple scattering need be applied.

The accuracy and applicability of equation 17 has been numerically checked against our *in-silico* reference bond length dependent PA-MFPADs of the CO^{2+} molecule detailed in the preceding paper [1]. We have demonstrated analytically that the EXAFS-like formula gives us the bond length of the dissociating CO^{2+} molecule with an accuracy of 0.05-0.1 Å.

This method will become applicable to experiments with the COLTRIMS–Reaction Microscope end station [19] installed in the SQS beam line of European XFEL [18] and the DREAM end station [35] equivalent to the COLTRIMS-Reaction Microscope installed in LCLS-II [20], when the two-color femtosecond soft XFEL starts operating for time-resolved studies in the near future [20, 21]. XFEL facilities usually have a femtosecond NIR laser systems that may be synchronized with XFEL pulses and thus used for orientating target molecules. Then, measurements for the forward-backward intensity ratios are straightforward and variations of the bond-length can be extracted from such measurements. We hope that time-resolved PA-MFPADs will become a new attractive pathway to make molecular movies visualizing intramolecular reaction.

Acknowledgement

We would like to acknowledge C. R. Natoli for fruitful discussions. This work was performed under the Cooperative Research Program of "Network Joint Research Center for Materials and Devices". K.H. acknowledges funding by JSPS KAKENHI under Grant No. 18K05027 and 17K04980. K. Y. is grateful for the financial support from Building of Consortia for the Development of Human Resources in Science and Technology, MEXT, and JSPS KAKENHI Grant Number 19H05628.

References

[1] Fukiko Ota, Kaoru Yamazaki, Didier Sébilleau, Kiyoshi Ueda, and Keisuke Hatada. Theory on polarization-averaged core-level molecular-frame photoelectron angular distributions: I. a full-potential method and its application to dissociating carbon monoxide dication. To be published in J. Phys. B: At. Mol. Opt. (this volume as Paper I).

[2] Ahmed H. Zewail. 4D visualization of matter: recent collected works. Imperial College Press, London, 2014. OCLC: ocn880965090.

[3] R.J. Dwayne Miller. Mapping Atomic Motions with Ultrabright Electrons: The Chemists' Gedanken Experiment Enters the Lab Frame. Annual Review of Physical Chemistry, 65(1):583–604, 2014. PMID: 24423377.

[4] P. Emma, R. Akre, J. Arthur, R. Bionta, C. Bostedt, J. Bozek, A. Brachmann, P. Bucksbaum, R. Coffee, F.-J. Decker, Y. Ding, D. Dowell, S. Edstrom, A. Fisher, J. Frisch, S. Gilevich, J. Hastings, G. Hays, Ph. Hering, Z. Huang, R. Iverson, H. Loos, M. Messerschmidt, A. Miahnahri, S. Moeller, H.-D. Nuhn, G. Pile, D. Ratner, J. Rzepiela, D. Schultz, T. Smith, P. Stefan, H. Tompkins, J. Turner, J. Welch, W. White, J. Wu, G. Yocky, and J. Galayda. First lasing and operation of an Ångstrom-wavelength free-electron laser. Nature Photonics, 4:641–647, 2010.

[5] S. P. Weathersby, G. Brown, M. Centurion, T. F. Chase, R. Coffee, J. Corbett, J. P. Eichner, J. C. Frisch, A. R. Fry, M. Gühr, N. Hartmann, C. Hast, R. Hettel, R. K. Jobe, E. N. Jongewaard, J. R. Lewandowski, R. K. Li, A. M. Lindenberg, I. Makasyuk, J. E. May, D. McCormick, M. N. Nguyen, A. H. Reid, X. Shen, K. Sokolowski-Tinten, T. Vecchione, S. L. Vetter, J. Wu, J. Yang, H. A. Dürr, and X. J. Wang. Mega-electron-volt ultrafast electron diffraction at SLAC National Accelerator Laboratory. Review of Scientific Instruments, 86(7):073702, 2015.

[6] M. P. Minitti, J. M. Budarz, A. Kirrander, J. S. Robinson, D. Ratner, T. J. Lane, D. Zhu, J. M. Glownia, M. Kozina, H. T. Lemke, M. Sikorski, Y. Feng, S. Nelson, K. Saita, B. Stankus, T. Northey, J. B. Hastings, and P. M. Weber. Imaging Molecular Motion: Femtosecond X-Ray Scattering of an Electrocyclic Chemical Reaction. Phys. Rev. Lett., 114:255501, Jun 2015.

[7] T. J. A. Wolf, D. M. Sanchez, J. Yang, R. M. Parrish, J. P. F. Nunes, M. Centurion, R. Coffee, J. P. Cryan, M. Gühr, K. Hegazy, A. Kirrander, R. K. Li, J. Ruddock, X. Shen, T. Vecchione, S. P. Weathersby, P. M. Weber, K. Wilkin, H. Yong, Q. Zheng, X. J. Wang, M. P. Minitti, and T. J. Martínez. The photochemical ring-opening of 1,3-cyclohexadiene imaged by ultrafast electron diffraction. Nature Chemistry, 11:504 – 509, 2019.

[8] F. Krasniqi, B. Najjari, L. Strüder, D. Rolles, A. Voitkiv, and J. Ullrich. Imaging molecules from within: Ultrafast angström-scale structure determination of molecules via photoelectron holography using free-electron lasers. Physical Review A, 81:033411, Mar 2010.

[9] Misato Kazama, Takashi Fujikawa, Naoki Kishimoto, Tomoya Mizuno, Jun-ichi Adachi, and Akira Yagishita. Photoelectron diffraction from single oriented molecules: Towards ultrafast structure determination of molecules using x-ray free-electron lasers. Physical Review A, 87:063417, Jun 2013.

[10] D. P. Woodruff. Photoelectron diffraction: from phenomenological demonstration to practical tool. Applied Physics A, 92:439–445, 2008.

[11] J. Ullrich, R. Moshammer, A. Dorn, R. Dörner, L. Ph. H. Schmidt, and H. Schmidt-Böcking. Recoil-ion and electron momentum spectroscopy: reaction-microscopes. Reports on Progress in Physics, 66(9):1463–1545, aug 2003.

[12] J. B. Williams, C. S. Trevisan, M. S. Schöffler, T. Jahnke, I. Bocharova, H. Kim, B. Ulrich, R. Wallauer, F. Sturm, T. N. Rescigno, A. Belkacem, R. Dörner, Th. Weber, C. W. McCurdy, and A. L. Landers. Imaging Polyatomic Molecules in Three Dimensions Using Molecular Frame Photoelectron Angular Distributions. Physical Review Letters, 108:233002, Jun 2012.

[13] Hironobu Fukuzawa, Robert R. Lucchese, Xiao-Jing Liu, Kentaro Sakai, Hiroshi Iwayama, Kiyonobu Nagaya, Katharina Kreidi, Markus S. Schöffler, James R. Harries, Yusuke Tamenori, Yuichiro Morishita, Isao H. Suzuki, Norio Saito, and Kiyoshi Ueda. Probing molecular bond-length using molecular-frame photoelectron angular distributions. The Journal of Chemical Physics, 150(17):174306, 2019.

[14] A Rouzée, P Johnsson, L Rading, A Hundertmark, W Siu, Y Huismans, S Düsterer, H Redlin, F Tavella, N Stojanovic, A Al-Shemmary, F Lépine, D M P Holland, T Schlatholter, R Hoekstra, H Fukuzawa, K Ueda, and M J J Vrakking. Towards imaging of ultrafast molecular dynamics using FELs. Journal of Physics B: Atomic, Molecular and Optical Physics, 46(16):164029, aug 2013.

[15] R. Boll, D. Anielski, C. Bostedt, J. D. Bozek, L. Christensen, R. Coffee, S. De, P. Decleva, S. W. Epp, B. Erk, L. Foucar, F. Krasniqi, J. Küpper, A. Rouzée, B. Rudek, A. Rudenko, S. Schorb, H. Stapelfeldt, M. Stener, S. Stern, S. Techert, S. Trippel, M. J. J.

ACCEPTED MANUSCRIPT

Vrakking, J. Ullrich, and D. Rolles. Femtosecond photoelectron diffraction on laser-aligned molecules: Towards time-resolved imaging of molecular structure. Phys. Rev. A, 88:061402, Dec 2013.

[16] Kyo Nakajima, Takahiro Teramoto, Hiroshi Akagi, Takashi Fujikawa, Takuya Majima, Shinichirou Minemoto, Kanade Ogawa, Hirofumi Sakai, Tadashi Togashi, Kensuke Tono, Shota Tsuru, Ken Wada, Makina Yabashi, and Akira Yagishita. Photoelectron diffraction from laser-aligned molecules with x-ray free-electron laser pulses. Scientific Reports, 5:14065, 2015.

[17] Shinichirou Minemoto, Takahiro Teramoto, Hiroshi Akagi, Takashi Fujikawa, Takuya Majima, Kyo Nakajima, Kaori Niki, Shigeki Owada, Hirofumi Sakai, Tadashi Togashi, Kensuke Tono, Shota Tsuru, Ken Wada, Makina Yabashi, Shintaro Yoshida, and Akira Yagishita. Structure determination of molecules in an alignment laser field by femtosecond photoelectron diffraction using an x-ray free-electron laser. Scientific Reports, 6:38654, 2016.

[18] Thomas Tschentscher, Christian Bressler, Jan Grünert, Anders Madsen, Adrian Mancuso, Michael Meyer, Andreas Scherz, Harald Sinn, and Ulf Zastrau. Photon Beam Transport and Scientific Instruments at the European XFEL. Applied Sciences, 7(6):592, Jun 2017.

[19] Gregor Kastirke, Markus S. Schöffler, Miriam Weller, Jonas Rist, Rebecca Boll, Nils Anders, Thomas M. Baumann, Sebastian Eckart, Benjamin Erk, Alberto De Fanis, Kilian Fehre, Averell Gatton, Sven Grundmann, Patrik Grychtol, Alexander Hartung, Max Hofmann, Markus Ilchen, Christian Janke, Max Kircher, Maksim Kunitski, Xiang Li, Tommaso Mazza, Niklas Melzer, Jacobo Montano, Valerija Music, Giammarco Nalin, Yevheniy Ovcharenko, Andreas Pier, Nils Rennhack, Daniel E. Rivas, Reinhard Dörner, Daniel Rolles, Artem Rudenko, Philipp Schmidt, Juliane Siebert, Nico Strenger, Daniel Trabert, Isabel Vela-Perez, Rene Wagner, Thorsten Weber, Joshua B. Williams, Pawel Ziolkowski, Lothar Ph. H. Schmidt, Achim Czasch, Florian Trinter, Michael Meyer, Kiyoshi Ueda, Philipp V. Demekhin, and Till Jahnke. Photoelectron Diffraction Imaging of a Molecular Breakup Using an X-Ray Free-Electron Laser. Physical Review X, 10:021052, Jun 2020.

[20] Joseph Duris, Siqi Li, Taran Driver, Elio G. Champenois, James P. MacArthur, Alberto A. Lutman, Zhen Zhang, Philipp Rosenberger, Jeff W. Aldrich, Ryan Coffee, Giacomo Coslovich, Franz-Josef Decker, James M. Glownia, Gregor Hartmann, Wolfram Helml, Andrei Kamalov, Jonas Knurr, Jacek Krzywinski, Ming-Fu Lin, Jon P. Marangos, Megan Nantel, Adi Natan, Jordan T. O'Neal, Niranjan Shivaram, Peter Walter, Anna Li Wang, James J. Welch, Thomas J. A. Wolf, Joseph Z. Xu, Matthias F. Kling, Philip H. Bucksbaum, Alexander Zholents, Zhirong Huang, James P. Cryan, and Agostino Marinelli. Photoelectron diffraction: from phenomenological demonstration to practical tool. Nature Photonics, 14:30–36, 2020.

[21] Svitozar Serkez, Winfried Decking, Lars Froehlich, Natalia Gerasimova, Jan Grünert, Marc Guetg, Marko Huttula, Suren Karabekyan, Andreas Koch, Vitali Kocharyan, and et al. Opportunities for Two-Color Experiments in the Soft X-ray Regime at the European XFEL. Applied Sciences, 10(8):2728, Apr 2020.

[22] J Korringa. On the calculation of the energy of a Bloch wave in a metal. Physica, 13(6):392 – 400, 1947.

[23] W. Kohn and N. Rostoker. Solution of the Schrödinger Equation in Periodic Lattices with an Application to Metallic Lithium. Physical Review, 94:1111–1120, Jun 1954.

[24] Francesco Aquilante, Jochen Autschbach, Rebecca K. Carlson, Liviu F. Chibotaru, Mickaël G. Delcey, Luca De Vico, Ignacio Fdez. Galván, Nicolas Ferré, Luis Manuel Frutos, Laura Gagliardi, Marco Garavelli, Angelo Giussani, Chad E. Hoyer, Giovanni Li Manni, Hans Lischka, Dongxia Ma, Per Åke Malmqvist, Thomas Müller, Artur Nenov, Massimo Olivucci, Thomas Bondo Pedersen, Daoling Peng, Felix Plasser, Ben Pritchard, Markus Reiher, Ivan Rivalta, Igor Schapiro, Javier Segarra-Martí, Michael Stenrup, Donald G. Truhlar, Liviu Ungur, Alessio Valentini, Steven Vancoillie, Valera Veryazov, Victor P. Vysotskiy, Oliver Weingart, Felipe Zapata, and Roland Lindh. Molcas 8: New capabilities for multiconfigurational quantum chemical calculations across the periodic table. Journal of Computational Chemistry, 37(5):506–541, 2016.

[25] L. S. Cederbaum, P. Campos, F. Tarantelli, and A. Sgamellotti. Band shape and vibrational structure in Auger spectra: Theory and application to carbon monoxide. The Journal of Chemical Physics, 95(9):6634–6644, 1991.

[26] D. Sébilleau, K. Hatada, H. F. Zhao, and C. R. Natoli. A Critical Assessment of Multiple Scattering Expansions. e-Journal of Surface Science and Nanotechnology, 10:599–608, 2012.

[27] J. J. Rehr, R. C. Albers, C. R. Natoli, and E. A. Stern. New high-energy approximation for x-ray-absorption near-edge structure. Physical Review B, 34:4350–4353, Sep 1986.

[28] Christiane P. Koch, Mikhail Lemeshko, and Dominique Sugny. Quantum control of molecular rotation. Rev. Mod. Phys., 91:035005, Sep 2019.

[29] Jian Wu and Heping Zeng. Field-free molecular orientation control by two ultrashort dual-color laser pulses. Phys. Rev. A, 81:053401, May 2010.

[30] G. G. Paulus, F. Grasbon, H. Walther, P. Villoresi, M. Nisoli, S. Stagira, E. Priori, and S. De Silvestri. Absolute-phase phenomena in photoionization with few-cycle laser pulses. Nature, 414(6860):182–184, Nov 2001.

[31] Yuxi Fu, Kotaro Nishimura, Renzhi Shao, Akira Suda, Katsumi Midorikawa, Pengfei Lan, and Eiji J. Takahashi. High efficiency ultrafast water-window harmonic generation for single-shot soft x-ray spectroscopy. Communications Physics, 3(1):92, May 2020.

[32] Tetsuo Katayama, Shigeki Owada, Tadashi Togashi, Kanade Ogawa, Petri Karvinen, Ismo Vartiainen, Anni Eronen, Christian David, Takahiro Sato, Kyo Nakajima, Yasumasa Joti, Hirokatsu Yumoto, Haruhiko Ohashi, and Makina Yabashi. A beam branching method for timing and spectral characterization of hard x-ray free-electron lasers. Structural Dynamics, 3(3):034301, 2016.

[33] Yoshiaki Kumagai, Hironobu Fukuzawa, Koji Motomura, Denys Iablonskyi, Kiyonobu Nagaya, Shin-ichi Wada, Yuta Ito, Tsukasa Takanashi, Yuta Sakakibara, Daehyun You, Toshiyuki Nishiyama, Kazuki Asa, Yuhiro Sato, Takayuki Umemoto, Kango Kariyazono, Edwin Kukk, Kuno Kooser, Christophe Nicolas, Catalin Miron, Theodor Asavei, Liviu Neagu, Markus S. Schöffler, Gregor Kastirke, Xiao-jing Liu, Shigeki Owada, Tetsuo Katayama, Tadashi Togashi, Kensuke Tono, Makina Yabashi, Nikolay V. Golubev, Kirill Gokhberg, Lorenz S. Cederbaum, Alexander I. Kuleff, and Kiyoshi Ueda. Following the birth of a nanoplasma produced by an ultrashort hard-x-ray laser in xenon clusters. Phys. Rev. X, 8:031034, Aug 2018.

[34] Daniel Rolles, Rebecca Boll, Benjami Erk, Dimitrios Rompotis, and Bastian Manschwetus. An Experimental Protocol for Femtosecond NIR/UV - XUV Pump-Probe Experiments with Free-Electron Lasers. JoVE, page e57055, 2018.

[35] `https://lcls.slac.stanford.edu/instruments/l2si`.

ACCEPTED MANUSCRIPT